E≋RS

Phase transformation, microstructure and mechanical properties of Si$_3$N$_4$/SiC composite

Jian-Feng Yang [a,*], Tatsuki Ohji [b], Tohru Sekino [c], Chun-Liang Li [c], Koichi Niihara [c]

[a]*Japan Science and Technology Corporation (JST), Nagoya, 463-8687, Japan*
[b]*National Industrial Research Institute of Nagoya (NIRIN), Shidami Human Science Park, 2268-1, Simo-Shidami, Moriyama-ku, Nagoya, 463-8687, Japan*
[c]*The Institute of Scientific and Industrial Research (ISIR), Osaka University, Ibaraki, Osaka, 567-0047, Japan*

Abstract

The influence of SiC fine particle dispersion on phase transformation, microstructure and mechanical properties of Si$_3$N$_4$ ceramics has been investigated. While the SiC dispersion simply decreased the densification, it caused complex effects on the phase transformation behavior; the transformation was enhanced at low temperatures but suppressed at high temperatures. Since the phase transformation is a nucleation-grain growth process of β-Si$_3$N$_4$, SiC particles plausibly enhance formation of a great number of β-Si$_3$N$_4$ nuclei due to the high Si$_3$N$_4$–SiC interfacial energy, but inhibit their further phase transformation and grain growth. The mean size and the aspect ratio of the obtained β-Si$_3$N$_4$ grains decreased as a result of the SiC dispersion, thus bringing about increased flexural strength and decreased fracture toughness. © 2001 Elsevier Science Ltd. All rights reserved.

Keywords: Composites; Mechanical properties; Phase transformation; SiC; Si$_3$N$_4$; Sintering

1. Introduction

It has been reported that homogeneous dispersion of SiC fine particles into Si$_3$N$_4$ grains or grain boundaries can substantially improve the mechanical properties.[1–3] For an example, Niihara has reported that a strength above 1.5 GPa was realized for an Si$_3$N$_4$/25 vol.% SiC nanocomposite using amorphous Si–C–N powders, and that the high strength was maintained up to 1400°C.[1] The mechanical performance of the Si$_3$N$_4$/SiC composites has been largely affected by microstructural factors including the Si$_3$N$_4$ grain sizes and their aspect ratios,[3] and, therefore, many efforts [4–7] have been devoted to the microstructure of Si$_3$N$_4$/SiC composites during sintering. Many of these studies were focused on the influence of SiC particles on the rod-like β-Si$_3$N$_4$ grain growth.[6,7] It has been well recognized that the migration of a Si$_3$N$_4$ grain boundary is substantially inhibited by inter-granular SiC particles. However, little attention has been paid to the influences of the SiC on the α–β phase transformation of Si$_3$N$_4$ except for a few studies,[1,5,8] and those were not always consistent with each other. The entire process of the α–β phase transformation is usually divided into nucleation of β-Si$_3$N$_4$ in an α-rich matrix, transformation from α to β phase, and rod-like grain growth of β-Si$_3$N$_4$.[9] Niihara et al. [1,10] proposed that the SiC particles can be nucleation sites for β-Si$_3$N$_4$ in Si$_3$N$_4$/SiC nanocomposites. This speculation was based on the results of microstructure observation; the amount of the intra-granular SiC nano sized particles is very small compared to that of the inter-granular ones and the interface around these SiC particles is clean without secondary phase. Park et al.[5] reported that nucleation of β-Si$_3$N$_4$ occurred on the surface of SiC particles and that heat treatment between 1400 and 1600°C had an apparent effect on the final microstructure and mechanical properties. On the other hand, Pan et al.[8] proposed a grain growth mechanism of β-Si$_3$N$_4$ where SiC particles are not involved with the nucleation. They indicated that the crystallographic orientations of the β-Si$_3$N$_4$ grains and the intra-granular SiC particles were observed to be somewhat related with each other, caused by the rotation of nano-sized SiC particles dur-

* Corresponding author. Tel.: +81-52-739-0156; fax: +81-52-739-0136.

E-mail address: yangjf@nirin.go.jp (J.-F. Yang).

ing the sintering process. The previous studies[11,12] also indicated that growth of β-Si$_3$N$_4$ grains was strongly dependent on their densification and α–β phase transformation. This microstructure formation has been known to have a large influence on the mechanical properties such as strength and fracture toughness. Thus, the investigation of the effects of the SiC particles on the densification and phase transformation is essential to evaluate the influences of SiC particles on the microstructure and mechanical properties.

This paper focuses upon the influence of SiC particle dispersions on the microstructure formation (densification, phase transformation, and grain growth) and mechanical properties, for Si$_3$N$_4$/SiC nanocomposites fabricated by pressureless sintering. The microstructure developments are investigated in a wide temperature range between 1400 and 1850°C, and the strength and fracture toughness are evaluated for the densified samples. The obtained mechanical properties are discussed in relation to the formed microstructure.

2. Experimental procedures

α-Silicon nitride powder (SN-9S, Denka Co., Ltd., Tokyo, Japan) was used as the starting powder. The powder has high purity, average grain size of 1.1 μm, specific surface area of 7.3 m^2/g and α-Si$_3$N$_4$ phase content of >92%. Major impurities including aluminum, calcium, and iron were reported to be <1200 ppm, and the oxygen content is < 2 wt.%. β-SiC powder (Ibiden Co. Ltd., Ogaki, Japan, Particle size: 80 nm) was added as the reinforcing phase, whose amounts were varied as 0, 5, 10, 20 and 30 vol.%. MgAl$_2$O$_4$ and ZrO$_2$ powders were used as the sintering additives, whose total amount was 15 wt.% with the ratio of MgAl$_2$O$_4$ and ZrO$_2$ being 1:1 by weight. Homogeneous mixtures were obtained by ball-milling in a polyethylene pot for 24 h in ethanol, using high purity Si$_3$N$_4$ balls (75% ϕ5 mm + 25% ϕ15 mm). After the slurry was dried, dry milling for another 4 h by big Si$_3$N$_4$ balls (ϕ15 mm) and sieving were performed. The resulting powder mixture was uniaxially pressed at 20 MPa before being cold isostatically pressed at 200 MPa. The green compacts were placed in a Si$_3$N$_4$ saggar within a carbon crucible and sintered with a graphite resistance furnace (FVPHP-R-5, Fujidempa Kogyo Co. Ltd., Osaka, Japan). A sample was heated up to a temperature between 1400 and 1850°C with a rate of 20 °C /min and was kept for 2 h at a nitrogen pressure of 0.6 MPa, followed by natural cooling. Temperatures were chosen with an interval of 50 or 100°C in this range. This sintering program is for investigating the densification and phase transformation behaviors at the specific temperature. In addition, some samples were sintered at 1750°C for 8 h with otherwise the same conditions, to evaluate

the mechanical properties of the resultant dense materials. These samples attained almost full densities,

Bulk densities were measured by an Archimedes method in distilled water. Crystalline phases of the sintered specimens were determined by X-ray diffractometry (XRD, 50 kV, 150 mA, RU-200B, Rigaku Co. Ltd., Japan). The 2θ angle scanning rate was 4°/min, and the identification of the phases present in the specimens was according to JCPDS (Joint Commit of Power Diffraction Standards) data. The weight fraction of β-Si$_3$N$_4$ ($\rho_{\beta/(\alpha\beta)}$) in the sintered body after sintering at different temperature was calculated on the basis of the two highest XRD peaks of α-Si$_3$N$_4$ and the two of β-Si$_3$N$_4$ proposed by Gazzara and Messier as follows:[13]

$$\rho_\beta/_{(\alpha+\beta)} = \frac{(I_{\beta(101)} + I_{\beta(210)})}{(I_{\beta(101)} + I_{\beta(210)} + I_{\alpha(201)} + I_{\alpha(210)})} \quad (1)$$

The specimens sintered at 1750°C for 8 h were machined to prepare test bars of 40×4×3 mm^3 according to JIS R1601 to measure the flexural strength. The tensile surface of the specimen was ground and polished to a mirror surface using alumina paste. After the tensile edges were beveled, the three-point bending strength (span 30 mm) was measured with a cross-head speed of 0.5 mm/min. After the bending tests, the fracture surfaces were carefully cleaned, and microstructural formation was characterized by scanning electron microscopy (SEM, Model S-5000, Hitachi Co., Japan). Indentations were made with a Vickers diamond pyramid on the polished surface with a load of 196 N for 15 s (AVK-C2, Akashi Co. Ltd., Japan). Fracture toughness was calculated from measurements of the crack length by using the equation given by Niihara et al.[14]

3. Results and discussion

3.1. Densification and phase transformation

Fig. 1 shows the relative densities of samples containing different SiC contents, sintered at temperatures between 1400 and 1850°C, for 2 h. The densification was substantially retarded by the SiC particle dispersions in the Si$_3$N$_4$/SiC composites. Fig. 2 shows the β-Si$_3$N$_4$ phase contents of the samples in Fig. 1. The SiC dispersions tended to enhance the α-β phase transformation below 1600°C, but retarded it above that temperature. The transformation was most activated around 1600°C and was almost completed at 1650–1700°C. These temperatures were shifted by about plus 30–40°C for the addition of 30 vol.% SiC.

According to the Kingery's model for liquid phase sintering,[15] there are three sequential processes: grain rearrangement, dissolution/reprecipitation, and grain growth. Sintering of Si$_3$N$_4$ ceramics using α-phase powder
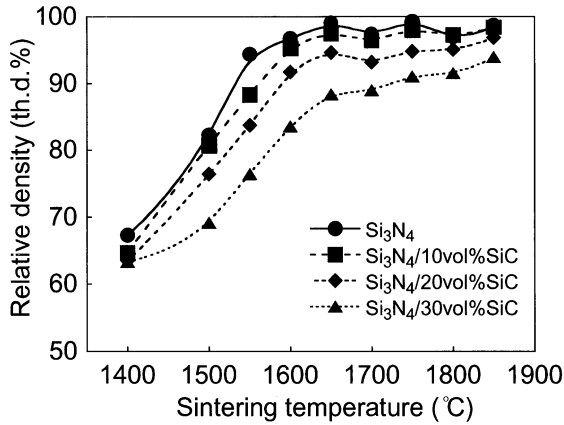
Fig. 1. Relative density versus temperature for monolithic Si_3N_4 and Si_3N_4-based composites containing 10, 20 and 30 vol.% SiC.
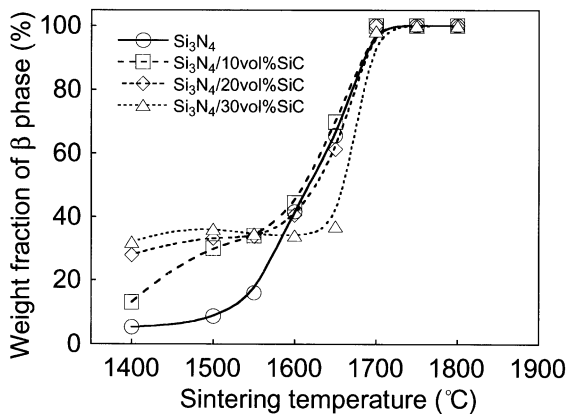

Fig. 2. Weight fraction of β phase Si_3N_4 versus temperature for monolithic Si_3N_4 and Si_3N_4-based composites containing 10, 20 and 30 vol.% SiC.

is always accompanied by some phase transformation from α- to β-Si_3N_4 along with the densification. However, although both the densification and transformation follow the same first-order kinetics and are rate-limited by grain boundary diffusion, their mechanisms are known to be basically different, particularly in the case of pressureless sintering.[16,17] The densification during liquid phase sintering is based mainly on grain rearrangement with some accommodation of the grain shape, while the α-β phase transformation is caused by dissolution of α-Si_3N_4 into boundary liquid and reprecipitation on β-Si_3N_4 grains. The suppressed densification due to the SiC additions is attributed to inhibition of the movement and accommodation of Si_3N_4 grains. On the other hand, the influence of SiC additions on the phase transformation was temperature-dependent. At the low temperatures, the phase transformation was prompted, however, at the high temperatures it was suppressed by the SiC particles, as shown in this study.

Generally, during normal sintering, the α-β Si_3N_4 phase transformation is suppressed by the SiC dispersion; the proportion of β-Si_3N_4 grains in Si_3N_4/SiC

composites after sintering decreases with the SiC content. This can be simply attributed to the suppressed mass transformation along the grain boundaries by the SiC particles, similarly to the inhibited grain growth.[3] The suppressed phase transformation observed at the high temperatures in this study corresponds to this. On the other hand, the phase transformation at the low temperatures is closely related with the β-Si_3N_4 nucleation. Two aspects should be considered for the nucleation of the β-Si_3N_4 grain; one is the number of nucleation sites and another is the surface energy. Grain boundary is usually the nucleation site, and an early study[18] showed that the critical energy required for the nucleation depends on the boundary types, four grain junctions making it easier to form secondary phase than the three and two grain junctions, due to the higher interfacial energy density. The Si_3N_4–SiC interfaces can be considered to have higher energy than the Si_3N_4–Si_3N_4 interfaces. One reason was that the SiC has a higher surface energy (several J/m^2)[19] than the Si_3N_4 (0.3 J/m^2)[20] originally caused by difference in the crystal structures. Another was the morphology of the SiC grains. It was noticed that the SiC particles in the Si_3N_4/SiC nanocomposites tend to be rounded, suggesting that interface energy of Si_3N_4–SiC was higher. The high surface energy implies a possibility that the Si_3N_4–SiC interfaces can act as β-Si_3N_4 nucleation sites, enhancing the phase transformation at low temperatures. It should be noted that the number of such Si_3N_4–SiC interfaces increases with increasing SiC content and temperature.

3.2. Microstructural formation and mechanical properties

Fig. 3(a)–(d) shows SEM micrographs of fracture surfaces of the monolithic Si_3N_4 and Si_3N_4/10, 20 and 30 vol.% SiC composites, sintered at 1750°C for 8 h. It should be noted that the matrix grain size and aspect ratio decreased substantially with increasing SiC content.

The final microstructure after α-β phase transformation strongly depends on the number and size of β-Si_3N_4 nucleation sites. It is known that a limited number of β phase seed particles, acting as the nuclei, leads to large elongated β-Si_3N_4 grains and improvement in fracture toughness.[21,22] In the previous section, the enhanced phase transformation at the low temperatures was considered to be due to the heterogeneous nucleation of β-Si_3N_4 at the Si_3N_4–SiC interfaces. The number of the Si_3N_4–SiC interfaces is so large that β-Si_3N_4 plausibly nucleates at many sites with a small size, leading to early impingement of β-Si_3N_4 during grain growth. In addition, further α–β phase transformation and subsequent β-Si_3N_4 grain growth at the high temperature was suppressed by the SiC addition. This combination gives rise to the refined microstructure as shown in Fig. 3. This is
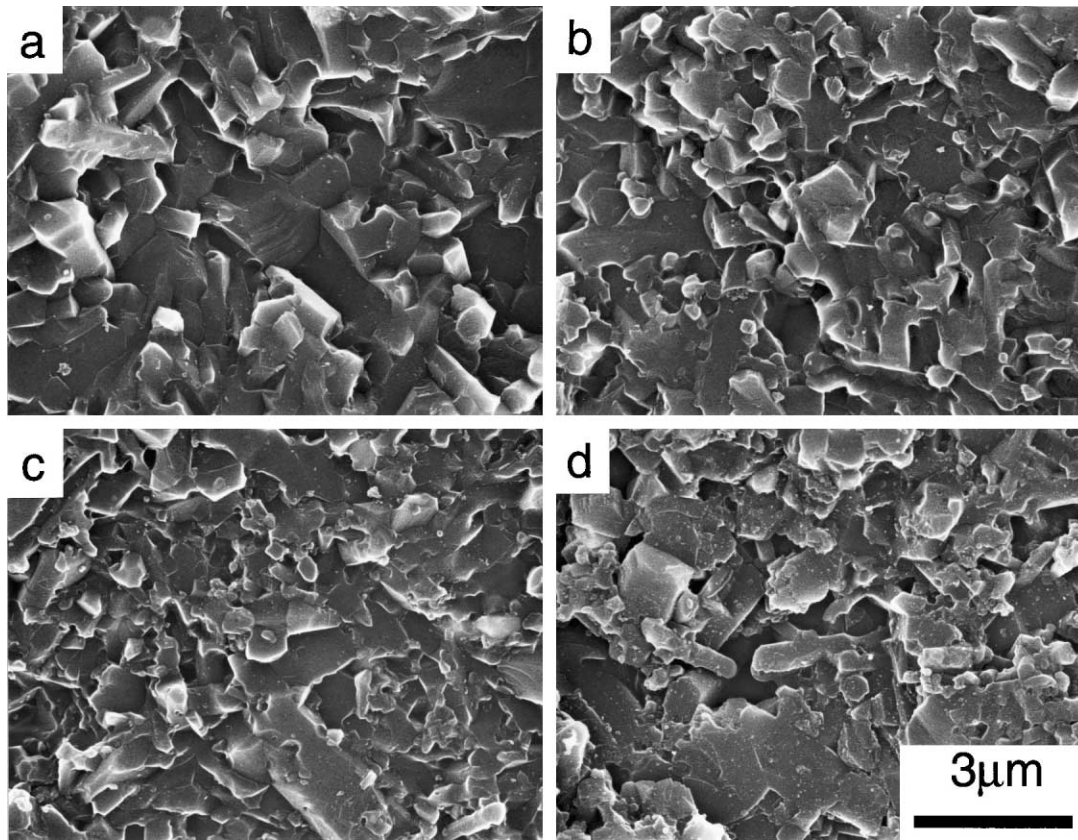
Fig. 3. SEM fracture surface of Si_3N_4–SiC composites. The samples were sintered at 1750°C for 8 h. The grain size of β-Si_3N_4 decreases with SiC content. (a) Si_3N_4; (b) Si_3N_4–10 vol.% SiC; (c) Si_3N_4–20 vol.% SiC; (d) Si_3N_4–30 vol.% SiC.
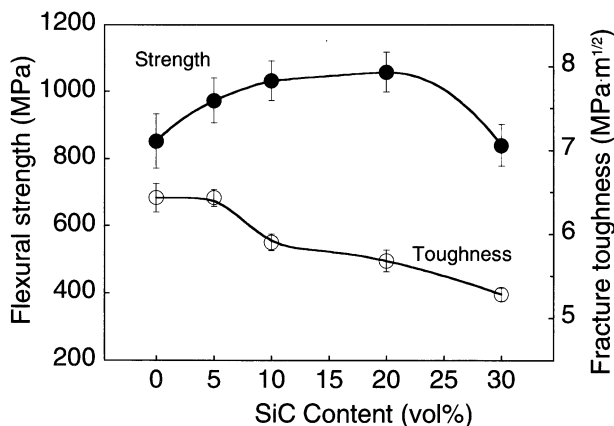

Fig. 4. Flexural strength and fracture toughness as functions of SiC addition.

similar to a finding by Park et al.,[15] who reported that a heat treatment at 1500°C before sintering resulted in a finer microstructure.

The flexural strength and fracture toughness of the composites are shown as a function of the SiC content in Fig. 4. As the SiC content increased, the fracture toughness monotonously decreased. On the other hand, the strength increased with increasing the content to a certain amount, but a further increase resulted in a drastic decrease of strength. The highest flexural strength of more than 1 GPa was obtained for a SiC content of 20 vol.%. The increased flexural strength and decreased fracture toughness by SiC addition are plausibly due to the refined microstructure. The low strength of the sintered composites at larger amounts of SiC addition is very likely caused by critical flaws associated with SiC agglomerates.[23]

4. Conclusion

The influences of SiC fine particle dispersion on phase transformation, microstructure and mechanical properties of Si_3N_4 ceramics have been investigated. While the SiC dispersion simply decreased the densification, it caused complex effects on the phase transformation behavior; the transformation was enhanced at the low temperatures but suppressed at the high temperatures. The enhancement was considered due to the formation of a great number of β-Si_3N_4 nuclei due to the high interfacial energy of the Si_3N_4-SiC interfaces, and the suppression was attributable to the degraded mass transformation ability brought about by the SiC particles. Due to the enhanced phase transformation at low temperature and the suppressed phase transformation at

the high temperatures, a refined microstructure could be formed, resulting in increased flexural strength and a reduced fracture toughness.

Acknowledgements

References

1. Niihara, K., New design concept of structural ceramics: ceramic nanocomposites. *J. Ceram. Soc. Jpn.*, 1991, **99**, 974–982.
2. Sternitzke, M., Review: structural ceramic nanocomposites. *J. Eur. Ceram. Soc.*, 1997, **17**, 1061–1082.
3. Hirano, T. and Niihara, K., Microstructure and mechanical properties of Si$_3$N$_4$/SiC composites. *Mater. Lett.*, 1995, **22**, 249–254.
4. Kondo, N., Suzuki, Y. and Ohji, T., Reaction-bonded and superplastically sinter-forged silicon nitride-silicon carbide nanocomposites. *J. Am. Ceram. Soc.*, 2000, **83**, 1816–1818.
5. Park, H., Kim, H. E. and Niihara, K., Microstructure and high-temperature strength of Si$_3$N$_4$-SiC nanocomposite. *J. Eur. Ceram. Soc.*, 1998, **18**, 907–914.
6. Herrmann, M., Schuber, C., Rendtel, A. and Aübner, H. H., Silicon nitride/silicon carbide nanocomposite materials: I, fabrication and mechanical properties at room temperature. *J. Am. Ceram. Soc.*, 1998, **81**, 1095–1108.
7. Yang, J. F., Choa, Y. H., Singh, J. P. and Niihara, K., Fabrication and mechanical properties of Si$_3$N$_4$/SiC nanocomposite with pressureless sintering and sinter-post-HIPing. *J. Ceram. Soc. Jpn.*, 1998, **106**, 951–957.
8. Pan, X., Mayer, J., Rühle, M. and Niihara, K., Silicon nitride based ceramic nanocomposite. *J. Am. Ceram. Soc.*, 1996, **76**, 585–590.
9. Krämer, M., Hoffmann, M. J. and Petzow, G., Grain growth studies of silicon nitride dispersed in an oxynitride glass. *J. Am. Ceram. Soc.*, 1993, **76**, 2778–2784.
10. Izaki, K., Nakahira, A. and Niihara, K., Si$_3$N$_4$/SiC nanocomposite from amorphous Si–C–N Powder Precursor. In *Proceedings of the 1st International Symposium on the Science of Engineering Ceramics*, ed. S. Kimura and K. Niihara. The Ceramic Society of Japan, Tokyo, Japan, 1991, pp. 443–.
11. Hirotsuru, H., Mitomo, M. and Nishimura, T., Relation between grain growth and phase transformation of silicon nitride. *J. Ceram. Soc. Jpn.*, 1995, **103**, 464–469.
12. Knoch, H., Schwetz, K. A. and Lipp, A., Microstructure development in silicon nitride. In *Progress in Nitrogen Ceramics*, ed. F. L. Riley. Martinus Nijhoff Publication, The Hague, The Netherlands, 1983, pp. 381–392.
13. Gazzara, C. P. and Messier, D. R., Determination of phase content of Si$_3$N$_4$ by X-ray diffraction analysis. *Am. Ceram. Soc. Bull.*, 1977, **56**, 777–780.
14. Niihara, K., Morena, R. and Hasselman, D. P. H., Evaluation of K_{IC} of brittle solid by the indentation method with low crack-to-indent ratios. *J. Mater. Sci. Lett.*, 1982, **1**, 13–16.
15. Kingery, W. D., Densification during sintering in the presence of liquid phase. *J. Appl. Phys.*, 1959, **30**, 301–312.
16. Yang, J. F., Ohji, T. and Niihara, K., Influence of yttria-alumina content on sintering behavior and microstructure of silicon nitride ceramics. *J. Am. Ceram. Soc.*, 2000, **83**, 2094–2096.
17. Park, J. Y., Kim, J. R. and Kim, C. H., Effects of free silicon on the α to β phase transformation in silicon nitride. *J. Am. Ceram. Soc.*, 1987, **70**, C240–C242.
18. Clemm, P. J. and Fisher, J. C., The influence of grain boundary on the nucleation of secondary phases. *Acta Metall.*, 1955, **3**, 70–73.
19. Kingery, W. D., Bowen, H. K. and Uhlmann, D. R., *Introduction to Ceramics*. Wiley-Interscience, New York, 1975.
20. Kitayama, M., Hirao, K., Toriyama, M. and Kanzaki, S., Modeling and simulation of grain growth in Si$_3$N$_4$. III. Tip shape evalution. *Acta Mater.*, 2000, **48**, 4635–4640.
21. Kanzaki, S., Brito, M. E., Valecillos, C., Hirao, K. and Toriyama, M., Microstructure designing of silicon nitride. *J. Eur. Ceram. Soc.*, 1997, **17**, 1841–1847.
22. Lu, H. and Huang, J., Microstructure in silicon nitride containing β-phase seeding. *J. Mater. Res.*, 1999, **14**, 2966–2973.
23. Sasaki, G., Nakase, H., Suganuma, K., Fujita, T. and Niihara, K., Mechanical properties and microstructure of Si$_3$N$_4$ matrix composite with nano-metre scale SiC particle. *J. Ceram. Soc. Jpn.*, 1992, **100**, 536–540.